



11th Conference of the International Sports Engineering Association, ISEA 2016

Comparison of IMU measurements of curling stone dynamics with a numerical model

Edward Lozowski^{a,*}, Sean Maw^b, Bernard Kleiner^c,

Krzysztof Szilder^d, Mark Shegelski^e, Petr Musilek^a, Dana Ferguson^a

^aUniversity of Alberta, Edmonton, T6G 2E3, Canada, ^bUniversity of Saskatchewan, Saskatoon, S7N 5A9, Canada, ^cUniversity of Calgary, T2N 1N4, Calgary, Canada, ^dNational Research Council, Ottawa, K1A 0R6, Canada, ^eUniversity of Northern British Columbia, Prince George, V2N 4Z9, Canada

Abstract

Despite almost a century of research, the question of what causes a curling stone to curl (move perpendicular to its initial direction of motion) has no complete answer. Many hypotheses have been formulated, but none has been able to account quantitatively for the full magnitude of the observed curl. The objective of this research was to equip a curling stone with an inertial measurement unit (IMU) and measure its motion, in order to verify a previously published, numerical model of curling stone dynamics. Low cost, small size, accuracy, ease of programming and operation, wireless data communication, and a data-sampling rate near 1 kHz, were selection criteria and constraints for the instrument package. We used the MicroStrain 3DM-GX4-25 system. This is a MEMS-based IMU with a tri-axial gyroscope and a tri-axial linear accelerometer. It was mounted and interfaced with a Bluetooth transmitter, on a curling stone handle. The data were streamed to a host laptop and displayed graphically in real time. Post-processing of the data included filtering and time-integration in order to obtain linear and angular velocities, and displacements. We have compared our experimental results with trajectory data calculated using a previously published numerical model, based on a thermodynamic approach to ice friction. While the observed longitudinal and angular motions are captured reasonably well by the model (errors of about 5% or less), no curl is predicted by the model.

© 2016 The Authors. Published by Elsevier Ltd. This is an open access article under the CC BY-NC-ND license (<http://creativecommons.org/licenses/by-nc-nd/4.0/>).

Peer-review under responsibility of the organizing committee of ISEA 2016

Keywords: curling; inertial measurement unit; numerical model; ice friction

1. Introduction

The sport of curling has experienced a resurgence of public interest, since it was re-introduced as a full Olympic sport in Nagano, in 1998. Although scientific investigations of curling dynamics go back almost a century [1], the past two decades have seen a resurgence of interest in the science of curling. Two recent papers [2,3] review the scientific history and current state-of-the-art. There are several published qualitative explanations of the physical cause of the curl. However, no quantitative model, based only on first principles, predicts the full dynamics of a curling stone. A complete model could be of practical value to coaches, curlers in training, and developers of curling game simulators.

Quantitative measurements of curling dynamics have been made by a number of authors using film and digital video [4,5]. These optical methods have used sampling frequencies (frame capture rates) of about 30 Hz, although the data were sometimes analyzed at rates of only 1-2 Hz. Because we suspected that measurements of curling stone dynamics at much higher sampling rates might reveal clues to the physics of the curl, we instrumented a curling stone handle and made a series of measurements in summer 2015. The objectives of this paper are 1. to describe the instrumentation, 2. to present some initial kinematic measurements, and 3. to compare the measurements with a new numerical model.

* Corresponding author. Tel.: +1-403-651-1456
E-mail address: Edward.Loizowski@ualberta.ca

2. Method

2.1 Instrumented curling stone handle

The dynamic behavior of a curling stone is the result of its interaction with many individual ice pebbles. The pebble encounter frequency is on the order of 1 kHz. In order to examine the details of the individual interactions, a measurement system with a frequency response of at least 10 kHz would be necessary. Since the cost of such a system was prohibitive, we used a lower sampling rate. The MicroStrain 3DM-GX4-25 IMU is capable of operation at 921,600 baud. RS232 and Bluetooth bandwidth limitations allowed us to achieve sampling rates of 250 Hz (angular velocity) and 500 Hz (linear acceleration). The data were transmitted wirelessly and archived and displayed in real time on a Microsoft Surface Pro 3 at the side of the ice sheet.

We chose live streaming and recording of the data, so that we could quickly detect procedural and system errors and make any necessary changes. The system was small enough to mount on a curling stone handle, although the MicroStrain housing interfered somewhat with the curler's ability to hold and throw the stone. Mounting on the handle rather than on the stone allowed us to install the system on a stone that had been sitting on the ice. Hence, we could be sure that the stone's running band was initially at ice temperature. The MicroStrain sensor was bonded directly to the plastic of the curling stone handle, while the peripheral equipment (batteries, interface, Bluetooth) was mounted in an open box, affixed to the handle using Velcro. The handle may have damped some of the high frequency vibrations of the stone. Fig. 1 is a photograph of the configuration.

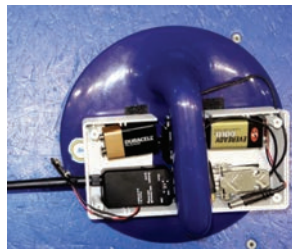


Fig. 1. MicroStrain system mounted on curling stone handle.

Inertial measurement units (IMU's) are electronic devices used to estimate a body's kinematics with respect to an initial condition, using accelerometers and gyroscopes. In principle, they can estimate a body's orientation and its linear and angular acceleration, velocity and displacement, all in 3D and as a function of time. Some IMU's also include magnetometers to help correct orientation drift. In a 3D unit, there is a separate linear accelerometer and a separate gyroscope for each axis. The accelerometers measure inertial accelerations, while the gyroscopes measure angular velocity.

A major challenge with IMU's is drift – the build-up of small systematic errors, as accelerations are integrated into velocities and then displacements. A systematic offset error in an accelerometer grows linearly in the velocity and quadratically in the displacement. It appears that there was some minor drift in our sensors, but this drift was largely compensated for, because it was systematic. An offset error was calculated in an initial quiescent and in a final quiescent state of the stone. The zero order and first order errors were then compensated for, using an assumption of temporal linearity.

For the experimental set-up in this study, the positive y-direction (longitudinal) was oriented along the longitudinal center of the ice sheet in the initial direction of motion of the stone, the positive x-direction (lateral) was oriented across the ice sheet to the right when looking down the ice, and the positive z-direction was vertical and oriented up out of the ice. This absolute coordinate system was fixed in the frame of reference of the ice. There are two other frames of reference that may be of value when discussing data and implications of results. Within the IMU, which is affixed to the stone, one can define a moving rectangular coordinate system, which we refer to as X, Y and Z, where Z and z are identical (except for imperfect leveling of the IMU and tipping of the stone). Positive Y and X are oriented forwards and to the right, relative to the stone and the IMU hardware. We record X and Y values and translate them into x and y values. We can also define a horizontal planar coordinate system related to the trajectory of the stone's center of mass. In this coordinate system, the y'-direction (forward) is tangent to the trajectory at any moment in time. The x'-direction (transverse) is perpendicular to the y'-direction and oriented to the right.

2.2 Measurements and data analysis

Our experiments were conducted at the curling rink in the University of Alberta Saville Centre. Because this is a national training facility, the ice and stones were well maintained. Our objective was to collect data over as wide a range of "realistic" conditions as possible. Our experimental protocol was divided into three regimes: 1. pure translational motion (no rotation), 2. pure rotational motion (no translation) and 3. combined translational and rotational motion, as seen in normal curling. Within the translational regime, we examined two translational speeds. Within the rotational regime, we examined two clockwise (CW)

rotational speeds and two counterclockwise (CCW) rotational speeds. Within the combined regime, we examined two values of translational speed, and three values each of CW speed and CCW speed. Here, we focus on the combined regime. The full set of 12 combined tests was conducted 3 times. That is, there were thirty-six tests corresponding to ordinary curling with combined rotation and translation.

In addition to recording and archiving the IMU output for each test, we also measured several other quantities: x- and y-coordinates of the stopping position of the stone, measured from the release point and the center line, respectively, using a tape measure; total number of rotations after release, estimated visually to the nearest 1/8 rotation by two independent observers; and slide time from release to stopping, using a stopwatch. In addition, we recorded videos of each throw using a camera mounted at the down-ice end of the rink. At this time, we can present only a small portion of this large archive of electronic and observational data, as analyses are ongoing.

One of the authors (DF) is an experienced curler and coach. DF made all of the stone throws. Each throw was launched as close as possible to the centerline with an initial velocity parallel to the centerline, but not necessarily precisely on the centerline. Throws were made so as not to have the stone collide with the bumpers surrounding the rink, in order to avoid damage to the instrumentation. We found that tests with nominally similar conditions were very similar in recorded behavior, even though they may have been made many tens of minutes apart. Table 1 illustrates the reproducibility and variability of the tests. Not surprisingly, slide time and y (the distance the stone moved longitudinally down the rink) and x (the distance the stone moved laterally on the rink) were correlated. Initial rotational velocity and total rotations were also correlated, though less so. The three cases C11, C29 and C47 were combined tests (ordinary curling) with fast initial CCW rotation and fast initial y-translation. While the three throws were not identical, their similarity (variability in slide time of $\pm 7\%$, for example) demonstrates the repeatability of the test conditions and outcome measures. Because of space limitations and the similarity of the three cases, we will show detailed results for case C11 only.

Table 1. Observed (bold) and calculated kinematic data for C11, C29 and C47.

	y (m)	v_{y0} (m/s)	x (m)	rotations (CCW)	rot_{init} (rad/s)	slide time (s)
C11	34.63	2.26	1.21	4.25	1.60	21.9
C29	37.06	2.35	1.24	4.88	1.67	23.3
C47	38.97	2.21	1.46	4.63	1.61	24.6

The raw signals from the IMU appear, at first glance, to be high amplitude, white noise. The accelerometer data, in particular, is dominated by high frequency oscillations (in the range of $\pm 1g$) produced by the interaction of the stone with individual pebbles. In order to extract the small linear accelerations associated with ice friction and curl, extensive post-processing in Excel™ was carried out.

Raw data files were low-pass filtered by applying a running 0.05 s averaging filter. The filtered Z gyro signal was then first order integrated to create a plot showing the total rotation during the throw of the rock. This calculated value was compared with visual observations recorded during experimentation. Typically, the computed results were within 45 degrees of the observed results. Note that the observed results were estimated and recorded to the nearest eighth of a rotation.

Realizing that the X and Y accelerometer values were taken from a rotating frame of reference on the curling rock throughout its motion, these X and Y values had to be converted into x and y accelerations, via a rotational transformation, using knowledge of when the X/Y and x/y axes were periodically aligned. In addition, the accelerometers experienced some minor drift over the course of the recordings. As noted earlier, this error was compensated for using a linear correction, based on values recorded before and after the movement of the rock.

With x and y acceleration for the rock determined with respect to time, these values were then integrated to get instantaneous x and y velocity with respect to time. Ideally, these data streams would begin and end at zero velocity. Typically, both velocities ended up being very close to zero.

Again using first-order integration, velocities were converted to positions to create plots of position with respect to time in both the lateral and longitudinal directions. Integration for the longitudinal position began at the last zero crossing on the longitudinal velocity plot, as that indicated the start of forward movement for the stone, after it was drawn back to begin the throw. The location where the rock stopped after the throw was recorded using a measuring tape, with an estimated accuracy of $\pm 0.01m$. However, the position on the rink where the forward motion began was known only approximately ($\pm 0.3 m$). This is because the release position of the stone was estimated using videos of the shot, taken from the end of the rink at eye level. Overhead cameras were not available. Our estimate of the error in release location results from the low camera angle and the difficulty in discerning precisely when the curler released her grip on the handle.

Similarly, integration for the lateral position began after the release of the rock, which was assumed to be the time at which the absolute value of the angular velocity peaked. Generally, the release took place close to the centerline of the rink. However, this was not highly controlled, leading to some minor noise in the results ($\pm 0.1 m$).

2.3 Numerical model

A detailed derivation of our numerical model of curling stone ice friction and dynamics was published in [2]. The model is based on “ordinary friction” interaction between the running band and the ice. The frictional interaction with individual pebbles is smoothed out around the perimeter of the running band. By “ordinary friction”, we mean friction that is proportional to the applied load and directed opposite to the velocity of a point on the running band relative to the stationary ice. The friction coefficient is derived based on two thermodynamic assumptions: 1. the ice/stone interface is at the pressure melting temperature and 2. the frictional energy is entirely dissipated by conduction into the ice and the stone. This approach originated with [6] and a similar derivation has been used in curling by others [4,7,8]. The friction coefficient between the running band and an ice pebble is calculated as a function of the relative velocity at the point of contact between the running band and a pebble, the ice hardness, the temperatures of the ice and stone surfaces, the thermal conductivity and thermal diffusivity of the ice and stone, the contact time of a point on the running band with the pebble and the contact time of a point on the pebble with the running band. The stone’s dynamic equations are based on 2D rotational, rigid body dynamics, as presented for example in [3]. Because of space limitations, we cannot present the full equations here.

The model initial conditions were the observed longitudinal and angular velocities at the instant of release of the stone by the curler. The initial lateral velocity was assumed to be zero in the model. The initial displacements were all set to zero in the model. In [2] we considered pure translation without rotation and then pure rotation. We did not consider combined translation and rotation. For the pure translation case considered in [2], the model error (compared with measurements in [4]) was 1 m for slide distance (4%) and 0.5 s for slide time (3%).

3. Results

The calculated velocity components (longitudinal v_y , lateral v_x , and rotational ω) are shown in Fig. 2a as solid blue lines, along with the corresponding modelled values (dashed red lines). The model-predicted displacements and measured displacements are shown in Fig. 2b. The time-dependent model curves in Fig. 2 were calculated from the model equations. The experimental curves in Fig. 2 were calculated from the IMU measurements and observed parameters.

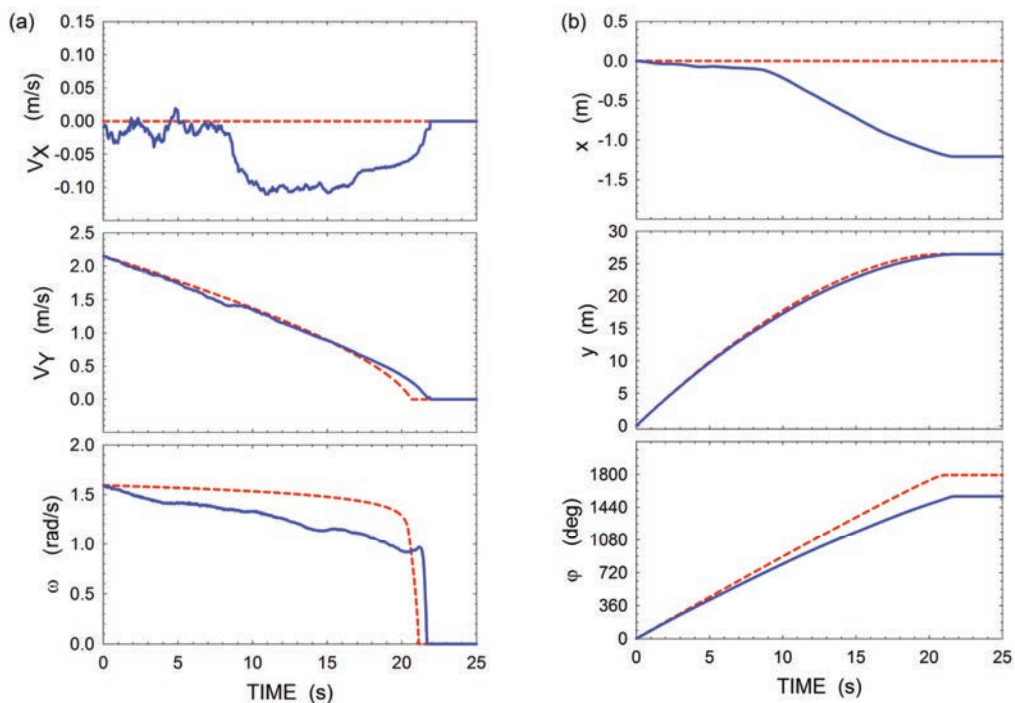


Fig. 2 Measured and model-predicted variables describing the dynamics and trajectory of a curling stone for Case C11. (a) x and y linear velocities and angular velocity of the stone as functions of time from the release point. (b) x and y displacement and angular displacement as functions of time from the release point. Red dashed curves are model predictions. Solid blue curves are derived from IMU measurements.

4. Discussion

For case C11 (Fig. 2), the model and experimental longitudinal velocities and stopping distances differ by less than 5%. This good agreement between model and experiment, already noted in [2], suggests that thermodynamically formulated “ordinary friction” can describe the longitudinal motion of curling stones quite well. Moreover, this agreement also supports the validity of the assumptions underlying the thermodynamic model of ice friction. In particular, the model assumes that the ice-stone interface is at the pressure melting temperature, implying the possibility of a thin melt layer of water at the interface. Because the friction model ignores squeeze flow, it also suggests that, unlike in higher speed sliding sports [9], squeeze flow is negligible for curling ice friction. This in turn implies that the lubricating liquid water layer is very thin. Unfortunately, the thermodynamic model conceals the detailed physics of the friction mechanism.

Our observations in Fig 2 reveal dynamics behavior that, to the best of our knowledge, has not been previously noted in the literature. Although this figure is for the single case of C11, cases C29 and C47 exhibit similar behavior. Briefly, for the first eight seconds after release, the lateral velocity is relatively low but fluctuating. Its magnitude averages around .01 m/s. Then the lateral velocity (perpendicular to the initial direction of motion) suddenly increases, rapidly at first and then more slowly, achieving a fluctuating value around 0.1 ms^{-1} , which is maintained for about 7 seconds. The final 5 seconds are characterized by a deceleration to zero lateral velocity, at first rapidly, then slowly and finally rapidly again. An examination of the numerical data shows that the rapid acceleration near 8 seconds is about 0.1 m/s^2 . This is comparable in magnitude to the deceleration in the longitudinal velocity and it is further evidence that “ordinary friction” cannot be the mechanism that gives rise to the curl. The lateral displacement curve shows that most of the curl occurs during the interval following this rapid lateral acceleration event. Similar events have been observed before [4], although they were not noted by the authors of the original paper. They are apparent only after re-analysis of the original data.

The fact that a quasi-constant lateral velocity (from about 8 to 15 s in Fig. 2) has been observed in two independent experiments ([4] and this paper), undertaken years apart by different research teams, needs some explanation. Unless it is a mere coincidence, it suggests that the force components along the direction of motion of the rock (y' -direction) and perpendicular to it (x' -direction) combine to give this result. It is not obvious that a constant lateral velocity should occur a priori, even though the assumption was used in the semi-phenomenological model in [4], with good results. However, rapid lateral acceleration and a constant lateral velocity could be important clues to what is happening in the rock-ice interaction, beyond “ordinary friction”.

Because frictional torque is produced by the same forces that give rise to longitudinal deceleration, one might expect better agreement between model and experiment than is observed. Others [1] have pointed out that the angular deceleration of a translating stone should be less than for a purely rotating stone, because the higher velocities imply lower friction coefficients. Moreover, the friction coefficient on the backward moving side of the stone is higher than that on the forward moving side of the stone, giving rise to a torque that tends to support the existing rotation. Hence, we should not be surprised that the angular deceleration is small over most of the trajectory in both model and experiment. However, it is significantly smaller in the model than in the experiments. This suggests that some other ice-stone interaction mechanism, beyond “ordinary friction”, is extracting energy from the angular motion of the stone. This mechanism can presumably also add energy to the angular motion, because Fig. 2a shows that the experimental angular velocity increases occasionally, although the total kinetic energy is a monotonically decreasing function of time. The precipitous drop in the experimental angular velocity near the end of the motion could be associated with the disappearance of a lubricating liquid film. In the model, a similar rapid drop in angular velocity is associated with the very rapid increase in the friction coefficient, as the velocity tends to zero.

The failure of our “ordinary friction” model to predict any lateral motion (curl) is not surprising. Many others have alluded to it [10,11]. It is a consequence of the front-back symmetry of the ordinary friction force. Maeno [3] has summarized several proposed qualitative mechanisms that could possibly give rise to an asymmetrical (front-back) friction mechanism, but none has yet been quantified and found to fit all existing observations of curling stone behavior. Maeno suggests that the curl may arise from a combination of mechanisms. At present, the ultimate physical explanations for the curl remain a subject of speculation. Nyberg et al. [11] were inadvertently misquoted in [2]. They did not show that “no anisotropic friction mechanism can explain the observed motion of a real curling stone.” [2]. Rather, “an isotropic friction mechanism, distributed asymmetrically around the circumference of the stone running band (by whatever mechanism), will never be able to produce the observed motion.” [12].

5. Conclusions

Our conclusions are summarized below:

- An IMU-based instrumented curling handle can be mounted on a competition curling stone and can be used to measure stone kinematics at a frequency between 250 Hz and 500 Hz.
- A numerical model of curling stone dynamics, based on a thermodynamic model of ice friction, has been verified by comparing model and experimental velocity and displacement data.
- The longitudinal kinematics predicted by the model agree well with the measurements, in terms of rate of deceleration and stopping distance and time. In the single case considered in this paper, the model and experimental stopping distance and time agree to within about 5%.

- The angular kinematics predicted by the model are qualitatively similar to the observations, but the model rate of angular deceleration is too slow. Both model and experiments exhibit a precipitous drop in angular velocity near the end of the trajectory. The experiments reveal brief periods when the angular velocity of the stone actually increases. Future models will need to account for such behavior.
- In its present form, our numerical model is unable to predict the observed curl, or indeed any curl. This failure is attributed to the front-back symmetry of ordinary friction, which produces no net transverse frictional force on the stone.
- The observed curl behavior is characterized by a sudden and rapid increase in lateral velocity followed by a period of relatively constant lateral velocity. Most of the lateral displacement (curl) occurs after this sudden lateral acceleration. Any complete model of curling dynamics will need to account for both rapid lateral accelerations and a period of almost constant lateral velocity.
- Based on our observations, we suspect, like Maeno [3], that the unique dynamics of a curling stone may arise from two or more distinct rock-ice interaction mechanisms.

Future research directions may include some of the following goals:

- Complete the analysis of all 36 combined linear/rotational experiments. Examine some of the other data streams produced by the IMU, such as “yaw derivative”, and examine the non-filtered, high frequency data to determine what they might reveal about individual pebble encounters.
- Develop a theory for a possible ice-rock interaction mechanism that can couple angular and linear motions and fully reproduce the observed dynamic behaviors in Fig. 2.
- Extend the model to account for the mechanical and thermodynamic effects of sweeping (brushing the ice ahead of the stone in order to influence its trajectory).

Acknowledgements

Renz Ocampo got this project rolling by developing our first instrument package for a curling stone. It consisted of a MEMS-based IMU (LSM9DS0) with an Edison controller. Daniel Bubola, chief icemaker at the Calgary Curling Club, assisted with ice analysis and provided our first testing rock. Rob Krepps, head curling coach at the UofA Saville Centre, provided availability to competition-quality curling ice and rocks for our final experiments. Yves Hamelin, director of the Calgary Olympic Oval, provided us with access to hockey ice for testing our instrument packages. Prof. A. Morris, MRU, provided helpful advice about the MicroStrain IMU. Erik Jensen, UNBC, kindly provided helpful, supplementary experimental data. Garry Timco, Bob Frederking, Louis Poirier and Kenny Lozowski listened patiently and gave us helpful questions and feedback when we tried to explain our curling ideas to them. Canada’s Natural Sciences and Engineering Research Council (NSERC) provided financial support.

References

- [1] Harrington EL. An experimental study of the motion of curling stones. *Trans and Proc Roy Soc Canada* 1924;8:247-259.
- [2] Lozowski EP, Szilder K, Maw S, Morris A, Poirier L, Kleiner B. Towards a first principles model of curling ice friction and curling stone dynamics. *Proc 25th Int Ocean and Polar Eng Conf* 2015:1730-1738.
- [3] Maeno N. Curling. In: Braghin F, Cheli F, Maldifassi S, Melzi S, Sabbioni E, editors. *The engineering approach to winter sports*. New York: Springer; 2016. p. 327-347.
- [4] Jensen ET, Shegelski MRA. The motion of curling rocks: experimental investigation and semi-phenomenologica description. *Canadian J Physics* 2004; 82:791-809.
- [5] Hattori K, Tokumoto M, Kashiwazaki K, Maeno N. High-precision measurement of curl distance by digital image analysis. *Proceedings Symposium on Sport and Human Dynamics* 2014; B33:14-40. (in Japanese)
- [6] Evans DCB, Nye JF, Cheeseman KJ. The kinetic friction of ice. *Proc Roy Soc Lond* 1976; A347:493-512.
- [7] Penner AR. The physics of sliding cylinders and curling rocks. *American J Physics* 2001; 69:332-339.
- [8] Marmo BA, Blackford JR. Friction in the sport of curling. *Proc 5th Int Sports Eng Conf* 2004;1:379-385.
- [9] Lozowski EP, Szilder K, Maw S. A model of ice friction for a speed skate blade. *Sports Eng* 2013;16:239-253.
- [10] Maeno N. Dynamics and curl ratio of a curling stone. *Sports Eng* 2013;17:33-41.
- [11] Nyberg H, Hogmark S, Jacobson S. Calculated trajectories of curling stones sliding under asymmetrical friction: validation of published models. *Tribology Letters* 2013;50:379-385.
- [12] Nyberg H. private communication 2015.